Int. J. Heat Mass Transfer. Vol. 15, pp. 2535–2549. Pergamon Press 1972. Printed in Great Britain

FREE CONVECTION ALONG THE DOWNWARD-FACING SURFACE OF A HEATED HORIZONTAL PLATE

T. AIHARA
Institute of High Speed Mechanics, Tōhoku University, Sendai, Japan

Y. YAMADA
Division of Engineering of Graduate School, Tōhoku University, Sendai, Japan

and

S. ENDŌ
Institute of High Speed Mechanics, Tōhoku University, Sendai, Japan

(*Received* 25 *August* 1971)

Abstract— An experiment has been made on quasi-two-dimensional, free convection heat transfer from a heated horizontal plate of Rayleigh number of the order of 10^7 in air; the velocity and temperature fields near the downward-facing surface have been measured. The velocity profile was found to be of the dual-flow type, and the possibility of obtaining similarity solutions for the present problem was also experimentally denied. The practically applicable range of boundary-layer approximation is discussed, and the local and average Nusselt numbers are compared with theoretical and experimental results reported by others.

NOMENCLATURE

a, one-half of the plate width [m, unless mentioned specially];
g, gravitational acceleration [m/s^2];
Gr, Grashof number, $g\beta(\theta_w - \theta_\infty)a^3/\nu^2$;
l, distance of two images of the same particle on a photograph [m];
m, magnification of an image on a photograph to the real object;
N, interception frequency of a rotating disk shutter [Hz];
Nu_x, local Nusselt number, $\alpha_x a/\lambda$;
Pr, Prandtl number;
Ra, Rayleigh number $Pr\,Gr$;
x, y, z, Cartesian coordinates [m, unless mentioned specially], see Figs. 1 and 2;
y_{max}, position of the maximum velocity [m, unless mentioned specially];
u, velocity in the x-direction [m/s, unless mentioned specially];
u_{max}, maximum velocity in the x-direction [m/s];
α_x, local heat transfer coefficient [W/m^{2}degC];
β, thermal expansion coefficient [1/degC];
δ_{inv}, position of the inversion layer [m];
δ_t, thickness of the thermal boundary layer defined as distance from plate at which $\phi = 0{\cdot}02$ [m];
δ_{th}, theoretical thickness of the boundary layer [m];
δ_1, stationary-layer thickness defined by equation (5) [m];
δ_4, boundary-layer thickness in the bi-quadratic-equation approximation of temperature profile [m];
θ, temperature [degC];
λ, thermal conductivity [W/m degC];
ν, kinematic vescosity [m^2/s];

ϕ, dimensionless temperature, $(\theta - \theta_\infty)/(\bar{\theta}_w - \theta_\infty)$.

Subscripts

w, wall conditions;
∞, ambient conditions.

Superscript

$-$, average value.

1. INTRODUCTION

FROM the viewpoint of a convective motive force, free convection along the downward-facing surface of a heated horizontal plate* is a peculiar phenomenon. Namely, in the usual free convection the buoyancy force component directed tangent to the surface of a body acts as the convective motive-force; however, in the case of free convection along a horizontal plate, the hydrostatic pressure gradient in the direction normal to the plate is first induced, and then its horizontal gradient acts as the direct motive-force of convection, as pointed out by Yamagata [1]. Consequently, the boundary layer has the maximum thickness at the plate center and the minimum thickness at the plate edges.

From interest in such peculiarity, the present problem has been hitherto studied extensively. Namely, experimental investigations of free convection heat transfer from a square or rectangular plate have been carried out by Weise [2], Kraus [3], Saunders *et al.* [4], and Birkebak *et al.* [5]; as for the average heat transfer coefficient for the upper or the lower surface, an empirical formula of Fishenden *et al.* [6] is generally utilized. The theoretical study was initiated in 1955 by Sugawara and Michiyoshi [7]. Although they attempted an analysis in the style of Hermann by approximating geometrically the horizontal plate by an ellipse of large eccentricity, the convective motive-force adopted was different from the one for the horizontal plate. Subsequently, Stewartson [8] and more correctly Gill *et al.* [9] have shown that the similarity solutions can not be obtained for free convection along an isothermal or constant flux, heated downward-facing surface.† On the other hand, approximate solutions by integral method have been reported successively by Wagner [11], Singh *et al.* [12, 13], Clifton *et al.* [14], Yamagata [1], and Fujii *et al.* [15], avoiding the mathematical difficulty. The validity of these approximate solutions depends on the boundary condition at the plate edge and the velocity and temperature profiles assumed in the respective analyses; therefore, some experimental verifications are desirable. However, no experiment corresponding to the two-dimensional theory has been reported yet.

From the above-mentioned viewpoint, the present study has been carried out to investigate the laminar free convection along the downward-facing surface of an isothermal horizontal plate by measuring carefully the velocity and temperature fields, and to explore the practically applicable range of boundary-layer approximation and the possibility of obtaining a similarity solution. The experiment was made at two temperature levels with a plate 250 mm wide and 10 mm thick in air, contriving to obtain the two-dimensional flow possible.

2. EXPERIMENTAL APPARATUS AND PROCEDURE

2.1 *Test plate and free convection chamber*

Figure 1 illustrates the construction details of a test plate. A test plate ① was a rectangular brass plate with completely parallel surfaces of waviness of 30 μ, which had several long holes for inserting thermocouples and nichrome wires.

* Free convection along the upward-facing surface of a cold horizontal plate is phenomenally the same as the present problem; however, for convenience, the downward-facing heated surface alone will be considered in this report.

† As for an upward-facing heated surface, similarity solutions have been obtained [8–10], provided a stable laminar boundary layer exists.

A 0·32 mm dia. nichrome heater ④ insulated by porcelain tubes of 1 mm o.d. was inserted in the plate ① as shown in the figure; the inserting mouths were sealed with brass side-pieces ②, which were press-fitted to the plate ①, interposing soft copper foils 30 μ thick to reduce the thermal contact resistance. Through small holes in these side-pieces ②, the 0·32 mm dia. copper current leads ⑤ were brought out.

chamber ⑧ as shown in Fig. 2. The convection flow was restrained two-dimensionally by holding vertically flat plate glasses 2 mm thick ④ as side walls parallel to the short sides of the test plate ②. The velocity and temperature fields were measured over the xy plane at $z = 0$; this plane will be designated "test cross-section" in the following. The thickness of insulation pieces ③ interposed between the

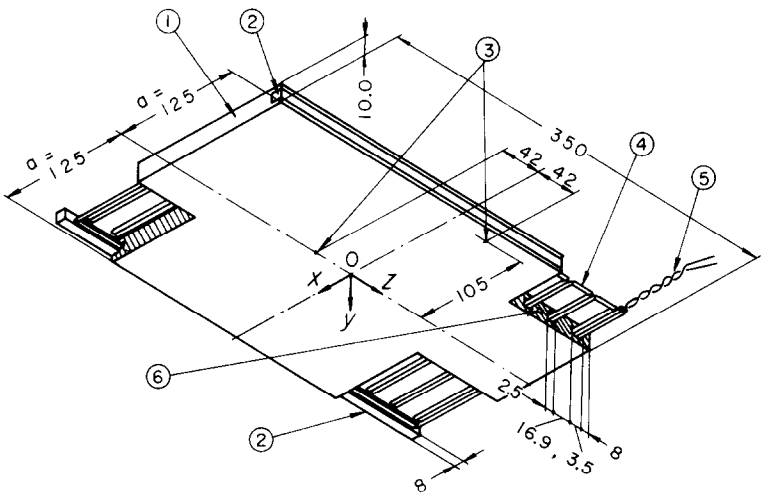

FIG. 1. Sectional details and characteristic length of test plate (units of dimensions: millimeters).

The preliminary measurements of the temperatures at twenty-five representative locations on both the upper and lower surfaces of the test plate showed that the temperature distributions were within 0·8 per cent of $(\bar{\theta}_w - \theta_\infty)$ over the range of $-1 < z/a < 1$ at two temperature levels. On the basis of this fact that the isothermal condition was almost satisfied, the average plate temperature $\bar{\theta}_w$ in the subsequent experiment was estimated from the measured values of 0·1 mm dia. copper–constantan thermocouples ③ embedded at two locations on the lower surface of the plate. The lead wires of these thermocouples were insulated by porcelain tubes, and brought out through small holes ⑥ in the plate ①.

The test plate was suspended horizontally within a slope of $\pm 10^{-4}$ in a wooden convection

side walls and the test plate were successfully adjusted, about 3 mm, so as to make the vertical temperature distribution of the plate glasses ④ equal to that of the convection flow and to reduce a secondary flow due to the side walls. Consequently, the almost satisfactory two-dimensional flow was obtained on and near the test cross-section as shown in Fig. 3 of streamline photographs, which were taken by the method described in Section 2.2 with a light beam parallel to the z-axis.

Ambient air temperatures θ_∞ in the convection chamber were measured with a 50 μ dia. copper–constantan thermocouple at a position 91 mm below the test plate; the vertical gradient of θ_∞ was within 0·0015°C/mm for $y < 0{\cdot}9$ m according to the preliminary experiment. These temperatures were measured to an accuracy of

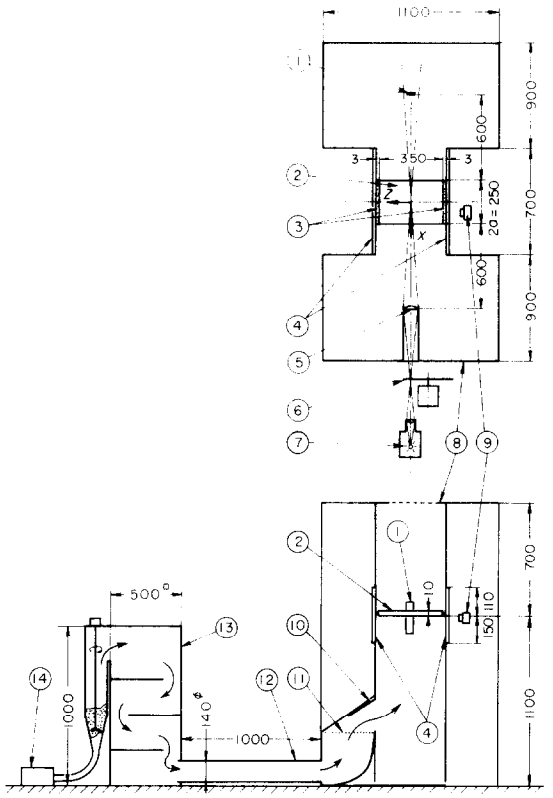

FIG. 2. Arrangement of velocity-measuring apparatus and convection chamber (units of dimensions: millimeters).

0·1°C by a d.c. potentiometer and a galvanometer.

2.2 *Measurement of velocity field*

The velocity field was measured by utilizing photographs of the trajectories of fine particles. As shown in Fig. 2, after thermal equilibrium was established, fine zinc stearate particles were suspended in air by a stirring type, continuous fluidized bed ⑬ and conducted through an acrylic-resin duct ⑫ into the convection chamber ⑧ at a low velocity of 5 mm/s for about 10 min. Then, the operation of an air blower ⑭ was stopped and a flap ⑩ was closed; the particles in the convection chamber were left to settle down under the gravity force for 60–90 min. The microphotographic observation indicated that the sizes of the majority of the remaining particles were within 2–6 μ after this procedure. In addition, the satisfactorily stable flow field could also be obtained by this settling procedure.

A light beam emitted by a super high pressure mercury lamp ⑦ (arc: 0·25 × 0·25 mm, average brightness: $1{\cdot}7 \times 10^5$ cd/cm^2) was intercepted periodically by a rotating-disk shutter ⑥ and focused on the plate center by a cylindrical lens ⑤ of 55 mm dia.; furthermore, a portion of this light beam was reflected by a plain mirror 5 mm wide ① so as to increase the intensity of light. Photographs of the trajectories of particles passing through this high-intensity light beam were taken on films with a speed of 400 A.S.A. with a camera ⑨ by using exposures of 1 s for measuring velocity and of 5–10 s for the flow pattern; and the development of films was sensitized enough (estimated at 4000 A.S.A.). At this time, the photograph of a 50 μ dia. constantan wire with three marking knobs stretched horizontally at a position 60 mm below the plate ② was simultaneously taken as a reference mark to determine the magnification of photograph m ($\doteqdot 2$) and the origin of coordinates (x, y). The rotating shutter ⑥ was a toothed disk which had several radial slots with a on–off ratio of 1:3 or 1:7 and was driven by a 20 W synchronous motor.

In order to restrain the effect of electrostatic field, the interior of the convection chamber was lined with aluminum foil, which was connected electrically with the test plate ②, a 120-mesh wire screen ⑪ and the apparatus for optical system ⑥⑦⑬ and then was earthed together. For the purpose of restraining stray reflection, this interior was further lined with flat black papers, and the inner surface of the side wall glass ④ opposite to the camera was painted black.

Figure 4 illustrates a typical photograph of the particle trajectories near the free edge obtained in the above-mentioned way. By measuring the distance l of two images (an average of three or four images in the case of

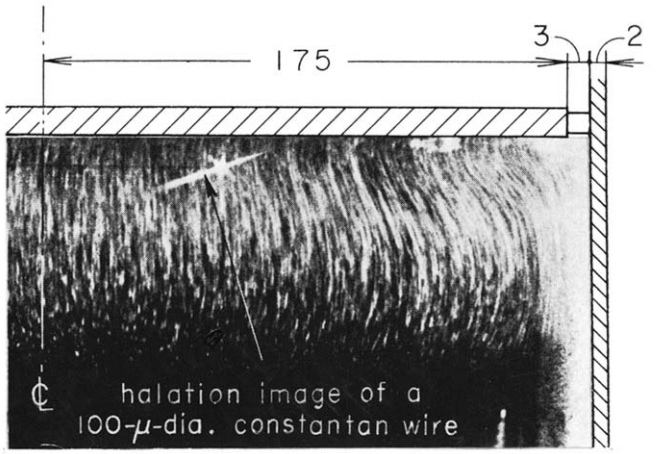

(a) along a cross-section at $x = a$.

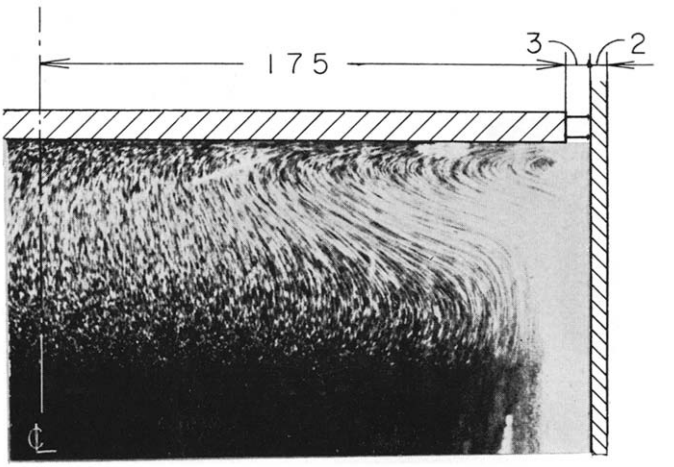

(b) along a cross-section at $x = a/2$.

FIG. 3. Photographs of the streamlines along a cross-section, parallel to the yz plane and perpendicular to the test cross-section.

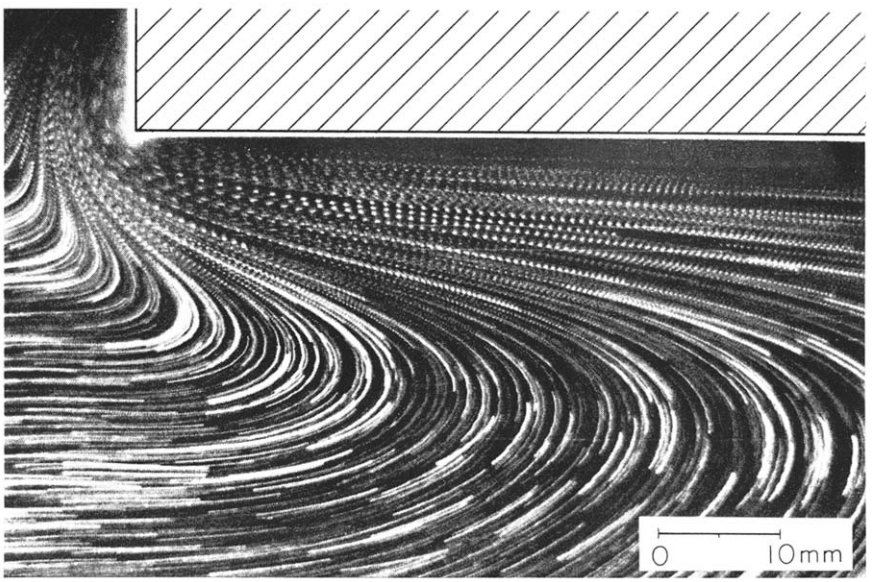

FIG. 4. Typical photograph of particle trajectories near the free edge of test plate ($\theta_w - \theta_\infty = 55{\cdot}2$ °C, interception frequency = 50 Hz, time of exposure = 1 s).

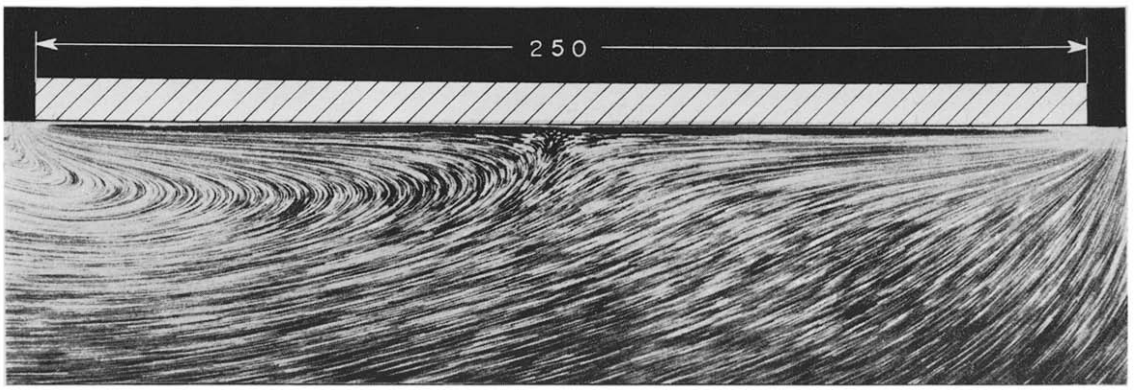

FIG. 6. Streamlines of a typical asymmetrical flow near the downward-facing surface ($\theta_w - \theta_\infty = 55{\cdot}2°C$, time of exposure = 1 s).

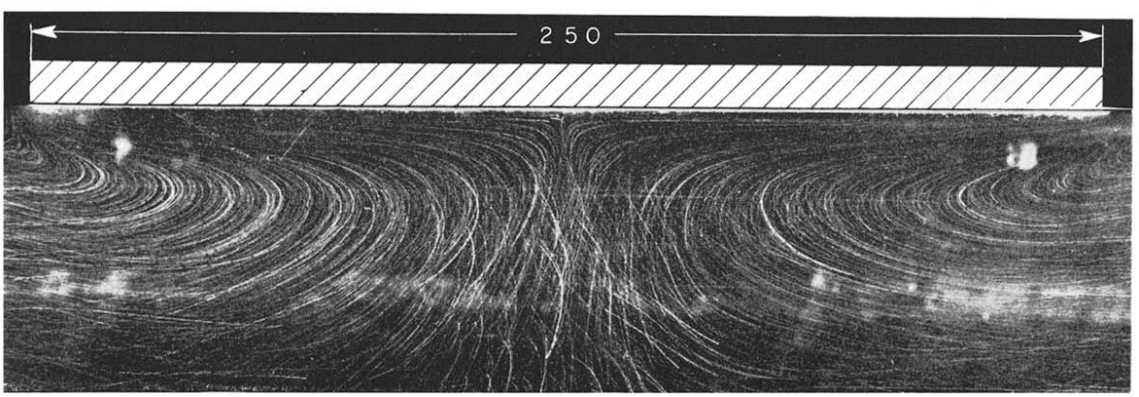

FIG. 7. Streamlines of a typical symmetrical flow near the downward-facing surface ($\theta_w - \theta_\infty = 55{\cdot}2°C$, time of exposure = 10 s).

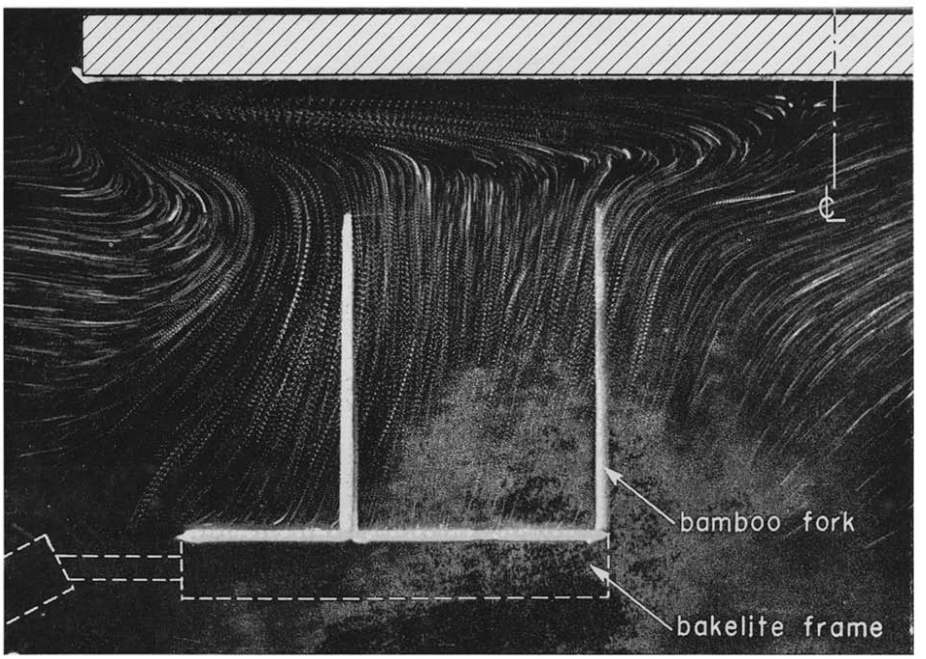

FIG. 21. Buoyant plume from a temperature probe ($\theta_w - \theta_\infty \doteq 100°C$).

low acceleration) of the same particle on such a photograph, the horizontal velocity u at the middle point can be determined by

$$u = lN/m, \quad (1)$$

where N is the interception frequency of the disk shutter, which was suitably selected from among 8·92, 25 and 50 Hz according to the particle velocity. The velocity at any point (x, y) is estimated by interpolation from the velocities for the two nearest points, on an assumption that the particles are constantly accelerating.

By the way, the maximum indeterminant error for the present measurements is predicted to be of the order of $\pm 0{\cdot}27$ per cent in x/a, of $\pm 0{\cdot}1$ mm in y, and of $\pm 5{\cdot}2$ per cent in u from the error analysis described in Appendix 1. However, since the average of the two or three measured values is used in the following analysis, the experimental scatter was much smaller than the above-mentioned errors.

2.3 *Measurement of temperature field*

It was first attempted to measure the temperature distribution in the boundary layer with a 25 μ dia. thermocouple stretched between bamboo forks attached to a bakelite frame, the construction details of which are described in reference [16]. However, since a buoyant plume from this bakelite frame disturbed remarkably the boundary layer as described in Appendix 2, such a method as shown in Fig. 5 was finally adopted to avoid the disturbance.

A 25 μ dia. chromel–alumel thermocouple ③ for temperature measurement was bonded at points B and B′ to 0·1 mm dia. enameled constantan wires ②, one end of which was joined to the closed end C of a 10 mm dia. stainless tube ①, and the other ends were pulled by dead weights (about 0·2 kg each) ④, touching the test plate ⑤ at points A and A′ and passing through standing blocks ⑥. The BB′-direction component of the tensile force acting on the constantan wires ② served to stretch the thermocouple ③ parallel to the test plate without sagging. The stainless tube ① was attached, through an airtight mechanism, to a vernier traverse-device with 1/50 mm division outside the test chamber so as to be capable of moving the thermocouple ③ without any disturbance. Its thermal electro-motive forces were printed on the strip-charts of a self-balancing electronic recorder against the occurrence of the so-called swaying motion.

Now, if the joint end of the constantan wires

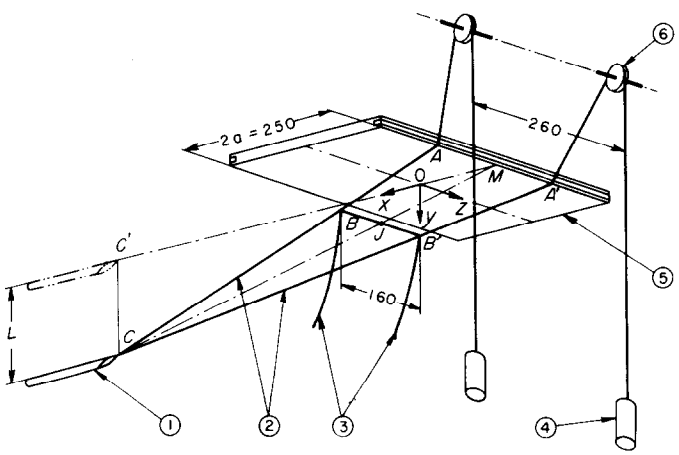

FIG. 5. Arrangement of temperature-measuring apparatus (units of dimensions: millimeters).

② is vertically moved down from point C′, at the same level as the origin 0, to a point C by a distance L, then the hot junction of thermocouple J moves to the position (x_j, y_j) given by

$$x_j = \overline{C'M} \cdot y_j/L - a, \tag{2}$$

$$y_j = L(1 - \overline{CJ}/\sqrt{[\overline{C'M}^2 + L^2]}), \tag{3}$$

where $\overline{CJ}$ and $\overline{C'M}$ are the line segment $\overline{CJ}$ and line segment $\overline{C'M}$ in Fig. 5 respectively. Therefore, as the hot junction J parts from the plate surface, the position of the hot junction x_j deviates from its initial position $x(= \overline{C'M} - a - \overline{CJ})$. Taking consideration of this point for the case of $\phi < 0{\cdot}6$, the temperature at any point (x, y) was estimated from dimensionless isotherms which were drawn by using the temperature data obtained in the above-mentioned way.

The maximum indeterminant error for these temperature measurements was predicted to be of the order of $\pm 0{\cdot}6$ per cent in boundary-layer temperature and of $\pm 0{\cdot}1$ mm in position (x, y).

3. RESULTS AND DISCUSSION

3.1 *Flow patterns near the downward-facing surface*

It was found that unlike the ordinary free convection around a body, the velocity field near the downward-facing surface of a horizontal plate is rather unstable, and that the completely symmetrical flow is not always obtainable over the whole region. Namely, the symmetry of the flow is apt to be marred by such disturbance sources as a faint "hot spot" as described in Appendix 2, an asymmetrical distribution of the wall temperature of the convection chamber, and a little slope of the test plate etc.*; in the worst case, the flow pattern becomes one as illustrated in Fig. 6. However, the flow in the boundary layer, particularly in the vicinity of the free edges, is comparatively stable; if such disturbance sources are got rid of by careful procedures, the nearly symmetrical flow can be attained over the whole region. So in the present report, the measured values for this symmetrical flow alone are adopted.

Figure 7 illustrates a typical symmetrical flow near the downward-facing surface. Some traces of a swaying motion [18, 19] occurring during an exposure time of 10 s are observed near the plate center $(x = 0)$; however, the majority of fluid flows almost horizontally from the right and left toward the plate center and flows out from the free edges after changing its course by 180° at the outer portion of the boundary layer. This "inversion of flow" seems to be peculiar to the heated downward-facing surface, because it was also observed on Birkebak *et al.*'s experiment [5] made with a downward-facing square plate with the vertical insulation walls on the edges in water. Then, a position near the plate at which the horizontal velocity u is zero will be termed "inversion layer" in the following.

3.2 *Velocity profiles and position of the inversion layer*

The velocity distributions were measured at two temperature levels of $(\bar{\theta}_w - \theta_\infty) = 55{\cdot}2$°C, corresponding to $Ra = 8{\cdot}20 \times 10^6$, and 104·0°C, corresponding to $Ra = 1{\cdot}17 \times 10^7$. The results are shown in Figs. 8 and 9; it may be seen that with increasing x/a, the position of inversion layer approaches the wall and the flow is accelerated. Solid curves in these figures are plots of Singh *et al.*'s approximate solution by integral method [13] expressed as

$$\left.\begin{aligned} u &= \frac{27}{4} u_{\max}\left(\frac{y}{\delta_{th}}\right)\left(1 - \frac{y}{\delta_{th}}\right)^2 && \text{for } y \leqq \delta_{th}, \\ u &= 0 && \text{for } y > \delta_{th}, \end{aligned}\right\} \tag{4}$$

where $u_{\max}$ is the maximum velocity, and δ_{th} the boundary-layer thickness. The measured position of the maximum velocity is considerably

* To an asymmetrical heated plate as reported by Fujii *et al.* [17], the corresponding flow is always asymmetrical.

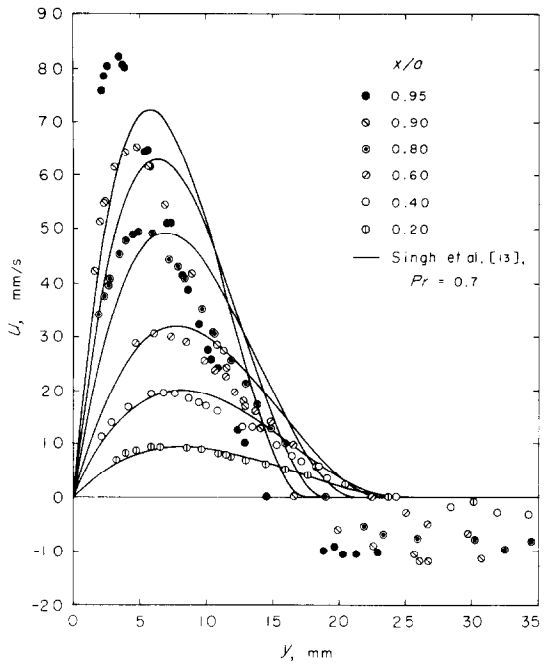

FIG. 8. Velocity profiles near the downward-facing surface ($\bar{\theta}_w - \theta_\infty = 55{\cdot}2°C$).

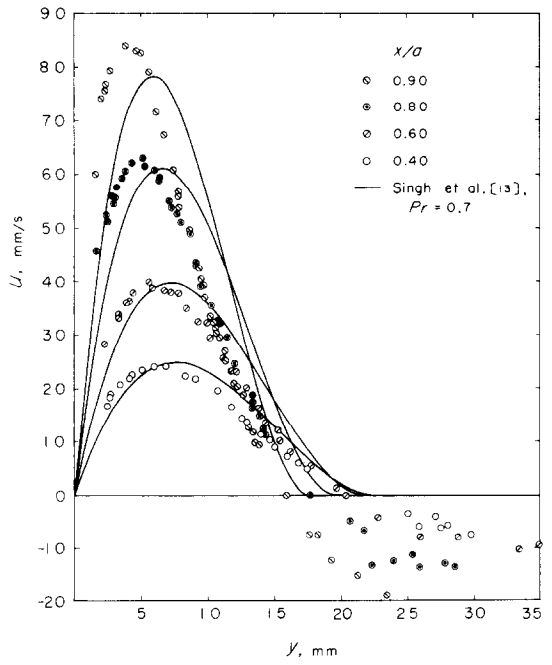

FIG. 9. Velocity profiles near the downward-facing surface ($\bar{\theta}_w - \theta_\infty = 104{\cdot}0°C$).

nearer to the wall than the theoretical position for every x/a, as may be seen from the figures. Such a tendency is usually observed in case of solving a free convection problem by integral method; however, the present tendency seems to be attributed partly to the fact of dual-flow* being neglected in their theory.

Figure 10 shows the maximum horizontal velocity u_{max} in a dimensionless form derived by examining the pertinent boundary-layer equations; the measured values become greater than the theoretical values on the basis of boundary-layer approximation as the x/a value exceeds about 0·8. The fluid properties in the present report are evaluated at the film temperature: $(\bar{\theta}_w + \theta_\infty)/2$, unless mentioned specially.

Figure 11 presents the respective distributions of the position of inversion layer δ_{inv} and the position of the maximum velocity y_{max}; with the use of these dimensionless groups, the effect of the temperature difference $(\bar{\theta}_w - \theta_\infty)$ almost disappears. It is noteworthy that in spite of the remarkable difference in y_{max} between the theory and the experiment, the measured positions of inversion layer δ_{inv} are nearly equal to the boundary-layer thickness, δ_{th}, obtained by integral method. The values of δ_{inv}/a in the present experiment are about 0·15 for $x/a = 0{\cdot}8$ and 0·09 for $x/a = 1$.

In Figs. 12 and 13, the velocity profiles are plotted in a dimensionless form based on the maximum velocity u_{max} and its position y_{max} obtained above. For the range of y/y_{max} less than about 1, it seems possible to represent the measured velocity profiles by a single average curve; however, for y/y_{max} greater than 1, no similarity between them appears to exist and the velocity profiles differ individually for each x/a and each Ra. It is particularly noteworthy that δ_{inv}/y_{max} tends to increase as x/a exceeds 0·6. These experimental facts support

* For example, a similar tendency has been also observed in the inversion flow near the lower stagnation point in free convection around a horizontal torus [20].

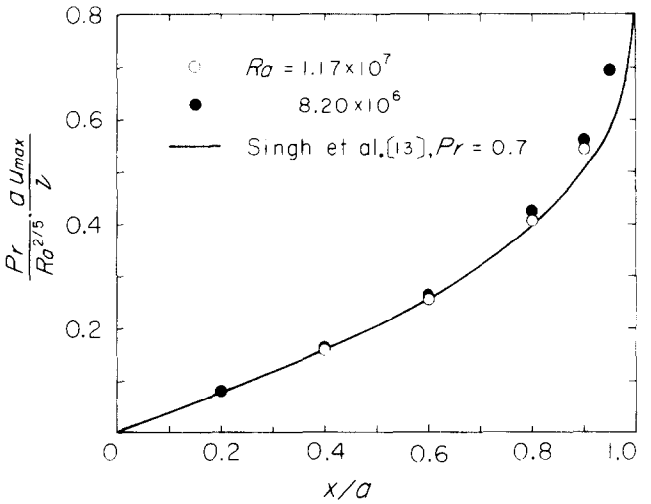

FIG. 10. Dimensionless maximum horizontal velocity vs. x/a.

the validity of Gill *et al.*'s theoretical conclusion [9] that the similarity solutions cannot be obtained for free convection along a downward-facing, isothermal, heated surface.

3.3 *Temperature field in the boundary layer*

The temperature distributions in the boundary layer were measured at two temperature levels of $(\bar{\theta}_w - \theta_\infty) = 52{\cdot}8°C$, corresponding to $Ra = 7{\cdot}16 \times 10^6$, and $101{\cdot}1°C$, corresponding to $Ra = 1{\cdot}02 \times 10^7$. Since a slow temperature oscillation, with the periods of about 33 s for the temperature difference 53°C and of about 25 s for 101°C, was observed in the boundary layer away from the wall, the time-average of these oscillating temperature data is used in the following analysis. The results are shown in Figs. 14 and 15; it may be seen that with increasing x/a, the boundary-layer thickness decreases in the same manner as in the velocity field.

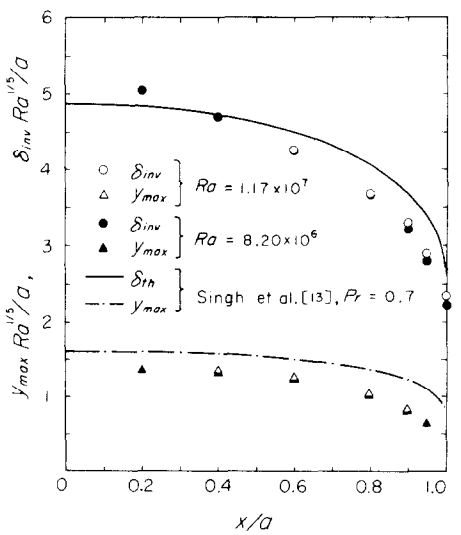

FIG. 11. Distributions of the respective dimensionless positions of the inversion layer and the maximum velocity.

In Figs. 16 and 17, the dimensionless temperatures ϕ are plotted against a dimensionless distance y/δ_1, where δ_1 is the stationary-layer thickness [21] defined by

$$\delta_1 = -(\bar{\theta}_w - \theta_\infty)/(\partial\theta/\partial y)_w. \qquad (5)$$

The temperature gradients at the wall $(\partial\theta/\partial y)_w$ are determined by approximating the temperature distributions for $\phi > 0{\cdot}7$ by the respective biquadratic equations. It may be seen in the figures that also in the temperature field, no similarity between the profiles for the vicinity of the free edge appears to exist. Solid curves in those figures are plots of the following poly-

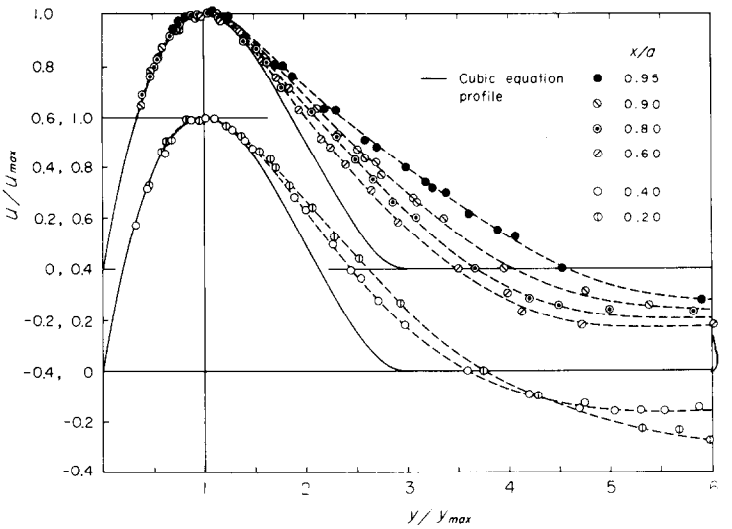

FIG. 12. Dimensionless velocity profiles in terms of u/u_{max} and y/y_{max} ($\bar{\theta}_w - \theta_\infty = 55{\cdot}2°C$).

nomials utilized usually in application of integral method:

$$\phi = (1 - y/\delta_2)^2 \qquad \text{with } \delta_2 = 2\delta_1, \tag{6}$$

$$\phi = (1 + y/2\delta_3)(1 - y/\delta_3)^2 \qquad \text{with } \delta_3 = 1{\cdot}5\delta_1, \tag{7}$$

$$\phi = (1 + y/\delta_4)(1 - y/\delta_4)^3 \qquad \text{with } \delta_4 = 2\delta_1. \tag{8}$$

It may be seen from the figures that excluding data for the region near the free edge, a bi-quadratic-equation approximation is best for representing the practical temperature distributions.

Figure 18 presents the respective x-direction distributions of the various thermal boundary-layer thicknesses in a dimensionless form derived by examining the pertinent boundary-

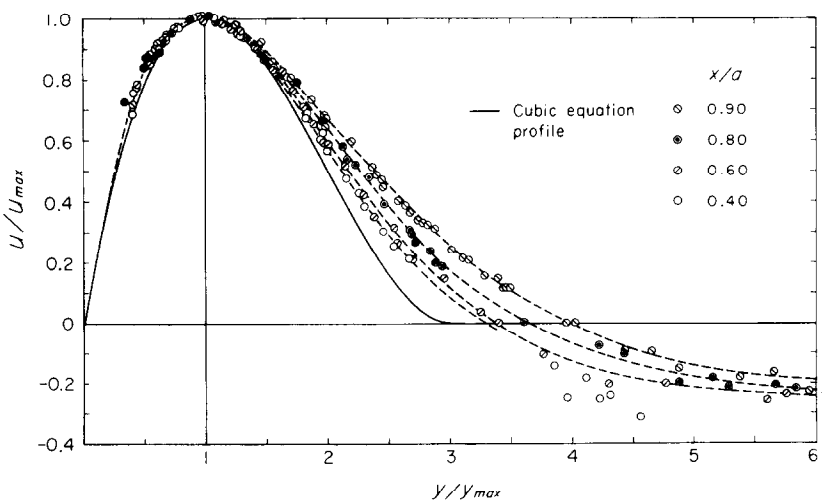

FIG. 13. Dimensionless velocity profiles in terms of u/u_{max} and y/y_{max}($\bar{\theta}_w - \theta_\infty = 104{\cdot}0°C$).

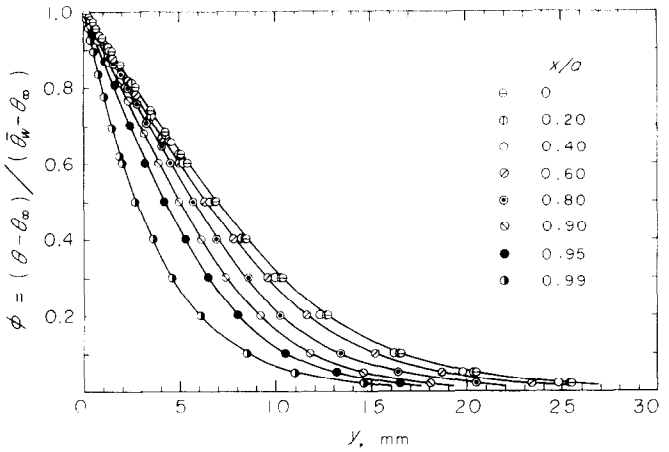

FIG. 14. Temperature profiles near the downward-facing surface ($\bar{\theta}_w - \theta_\infty = 52{\cdot}8°C$).

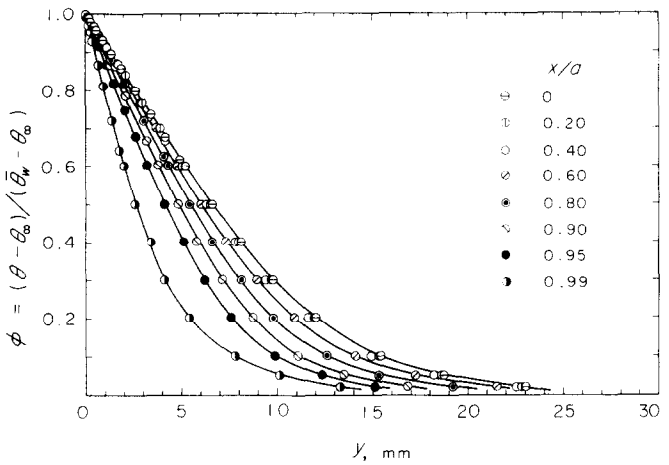

FIG. 15. Temperature profiles near the downward-facing surface ($\bar{\theta}_w - \theta_\infty = 101{\cdot}1°C$).

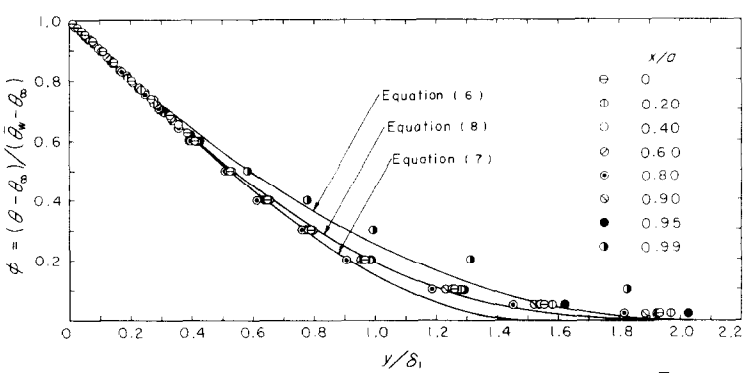

FIG. 16. Dimensionless temperature profiles in terms of ϕ and y/δ_1 ($\bar{\theta}_w - \theta_\infty = 52{\cdot}8°C$).

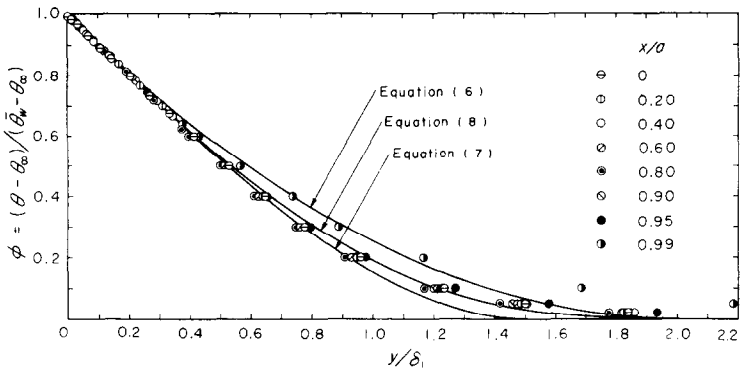

FIG. 17. Dimensionless temperature profiles in terms of ϕ and y/δ_1 ($\bar{\theta}_w - \theta_\infty$ = 101·1°C).

layer equations. In the figure, δ_4 is the boundary-layer thickness in the biquadratic-equation approximation of the temperature profile, and δ_t the thermal boundary-layer thickness defined as a distance from the plate at which $\phi = 0{\cdot}02$. Both measured boundary-layer thicknesses are nearly equal to the approximate solution δ_{th} according to Singh *et al.* [13]; however, δ_4 which is determined from the temperature gradient at the wall decreases rapidly in the vicinity of the free edge, as may be seen from the figure. This rapid decrease can be attributed to the effect of the x-direction conduction term which was neglected in their theoretical study; consequently, from further consideration of the similar tendency of the velocity field, it would seem that a substantially applicable limit of boundary-layer approximation is of the order of $\delta/(a - x) = 0{\cdot}8$ in the present problem. The unusual tendency, being reported by Rotem *et al.* [22], that the thermal boundary layer becomes thicker with increasing Ra cannot be observed in the present experiment, as may be seen from Fig. 18.

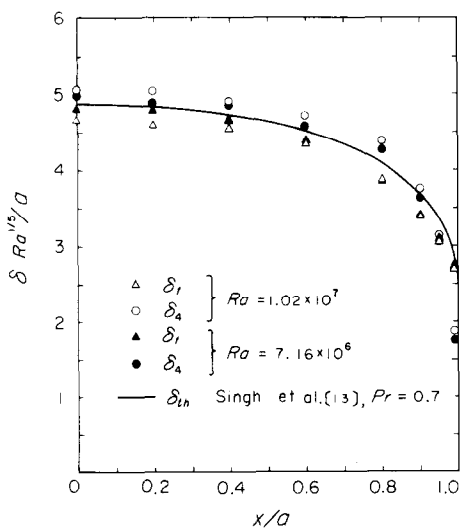

FIG. 18. Distributions of the various thermal boundary-layer thickness in the dimensionless from of $\delta\, Ra^{\frac{1}{5}}/a$ and x/a.

3.4 *Heat transfer coefficients*

The local heat transfer coefficient α_x can be evaluated from the above-mentioned δ_1 by setting $\alpha_x = \lambda_w/\delta_1$. The results are plotted against x/a in Fig. 19 in a dimensionless form of local Nusselt number Nu_x defined by

$$Nu_x = \alpha_x\, a/\lambda. \tag{9}$$

Singh *et al.*'s approximate solution by integral method [13] is also plotted in the same figure; the calculated local Nusselt number is somewhat smaller than the measured value, according to the fact that the calculated velocity is lower than the measured velocity in the vicinity of the wall (see Figs. 8 and 9). This tendency is especially prominent in the vicinity of the free edge, where the x-direction conduction term cannot be negligible. It is, however, of practical interest that in spite of the remarkable difference in the velocity profile between the theory and the experiment, both local Nusselt numbers are

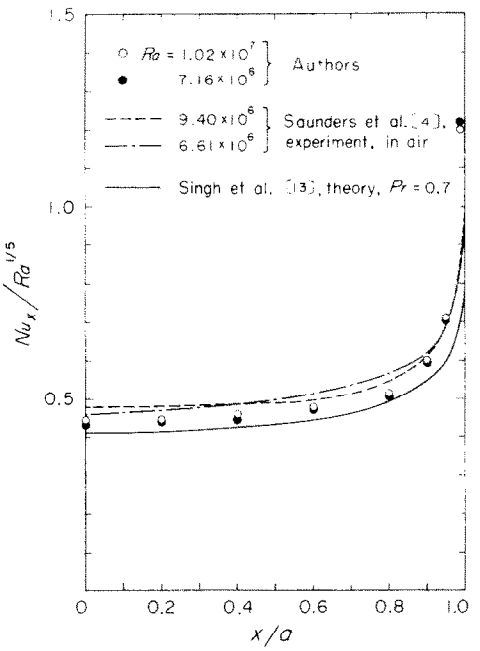

FIG. 19. Comparison of local Nusselt numbers Nu_x.

[4] on the lower surface of a rectangular plate 23 cm wide and 46 cm long are also plotted: their results are somewhat greater than the authors' data owing to a three-dimensionality of the flow.

Table 1 presents a comparison of the average Nusselt numbers obtained in the present experiment with results reported by others. Saunders *et al.*'s experimental values are obtained by integrating graphically the relevant curves in Fig. 19. Weise's data which were measured with a thermocouple stretched between forks [2], shows an extremely high value; this may be attributed to the buoyant plume as described in Appendix 2 and to some disturbance in traversing operation of the forks.

4. CONCLUSIONS

An experimental study has been made of quasi-two-dimensional, free convection heat transfer from the downward-facing surface of a horizontal plate with both surfaces heated; and the following conclusions are obtained:

(1) In free convection of a horizontal plate, the velocity field near the downward-facing surface is rather unstable; even faint thermal and hydrodynamic disturbances can be a source to mar the symmetry of the flow. However, in the boundary layer, particularly in the vicinity of the free edge, the flow is comparatively stable.

(2) In the case where a symmetrical flow is

Table 1. *Comparison of average Nusselt numbers* $\overline{Nu}$ *for the heated, downward-facing surface*

Investigators	$\overline{Nu}/Ra^{\frac{1}{4}}$	Remarks
Authors	0·509 for $Ra = 1{\cdot}02 \times 10^7$ 0·500 for $Ra = 7{\cdot}16 \times 10^6$	Experiment, quasi-two-dimensional flow, in air
Saunders *et al.* [4]	0·523 for $Ra = 9{\cdot}40 \times 10^6$ 0·526 for $Ra = 6{\cdot}61 \times 10^6$	Experiment, rectangular plate, in air
Weise [2]	0·864 for $Ra = 3{\cdot}42 \times 10^6$	Experiment, square plate, in air
Birkebak *et al.* [5]	0·681	Experiment, square plate, in water
Singh *et al.* [13]	0·460	Theory, two-dimensional flow, $Pr = 0{\cdot}7$

in comparatively good agreement over the major region of the plate. Namely, integral method can be regarded as a fairly effective means for the present problem also, in so far as the heat transfer coefficient is discussed. In Fig. 19, Saunders *et al.*'s experimental data*

* These data are the average values in the 46-cm direction which are evaluated from their Schlieren photographs by estimating the ambient temperature at 20°C by the authors. If a correction to the three-dimensionality of the boundary layer [23] is made, the values for the vicinity of the free edge will become larger.

obtained, an inversion region of the flow exists near the outer portion of the boundary layer and the velocity profile takes a form of dual-flow type. The position of "inversion layer" δ_{inv} at which the horizontal velocity is zero, is nearly equal to Singh *et al.*'s theoretical boundary-layer thickness δ_{th} by integral method; however, the measured position of the maximum velocity is considerably nearer to the wall than Singh *et al.*'s approximate solution.

(3) The validity of Gill *et al.*'s theoretical conclusion that the similarity solutions cannot be obtained for free convection along a downward-facing, isothermal, heated surface, is experimentally confirmed in both the velocity and temperature fields.

(4) Excluding data for the region near the free edge, a biquadratic-equation representation is best for approximating the temperature profile by a polynomial. The thermal boundary-layer thickness defined as distance from plate at which $\phi = 0{\cdot}02$ is nearly equal to the theoretical value δ_{th} over the whole region of the plate; however, the boundary-layer thickness in case of approximating the temperature profile by a biquadratic equation becomes considerably smaller than δ_{th} near the free edge.

(5) The measured values of the maximum velocity and local Nusselt number agree comparatively well with Singh *et al.*'s theoretical values by boundary-layer approximation for the region of $x/a < 0{\cdot}8$. However, the measured values for the vicinity of the free edge tends to be considerably greater than the theoretical values; it would seem that a substantially applicable limit of boundary-layer approximation is of the order of $\delta/(a - x) = 0{\cdot}8$ in the present problem.

ACKNOWLEDGEMENTS

The authors wish to express their gratitude to Professor T. Takeyama, Tōhoku University, for giving an opportunity for the present investigation, and for his continued advice and help, and to Professor Emeritus T. Tsubouchi, Tōhoku University, for his encouragement during this work.

REFERENCES

1. K. YAMAGATA. On the free convection from a horizontal surface. Proc. 6th Heat Transfer Symp. of Japan. pp. 73–76 (1969).
2. R. WEISE. Wärmeübergang durch freie Konvektion an quadratischen Platten. *Forsch. Ing.-Wes.* **6**. 281–292 (1935).
3. W. KRAUS. Temperatur- und Geschwindigkeitsfeld bei freier Konvektion um eine waagerechte quadratische Platte. *Phys. Z.* **41**, 126–150 (1940).
4. O. A. SAUNDERS, M. FISHENDEN and H. D. MANSION. Some measurements of convection by an optical method. *Engineering* 483–485 (May 1935).
5. R. C. BIRKEBAK and A. ABDULKADIR. Heat transfer by natural convection from the lower side of finite horizontal, heated surface. Preprints 4th Int. Heat Transfer Conf., Paris, 4. NC 2.2 (1970).
6. W. H. MCADAMS. *Heat Transmission*, p. 180. McGraw-Hill, New York (1954).
7. S. SUGAWARA and I. MICHIYOSHI. Heat transfer from a horizontal flat plate by natural convection. *Trans. Japan Soc. Mech. Engrs* **21**, 651–657 (1955).
8. K. STEWARTSON. On the free convection from a horizontal plate. *ZAMP* **9**, 276–282 (1958).
9. W. N. GILL, D. W. ZEH and E. DEL CASAL. Free convection on a horizontal plate. *ZAMP* **16**, 539–541 (1965).
10. Z. ROTEM and L. CLAASSEN. Natural convection above unconfined horizontal surfaces. *J. Fluid Mech.* **39**, 173–192 (1969), and Z. ROTEM and L. CLAASSEN. Free convection boundary-layer flow over horizontal plates and discs. *Can. J. Chem. Engng* **47**, 461–468 (1969).
11. C. WAGNER. Discussion on integral methods in natural convection flow. *J. Appl. Mech.* **23**, 320–321 (1956).
12. S. N. SINGH, R. C. BIRKEBAK and R. M. DRAKE, JR., Laminar free convection heat transfer from downward-facing horizontal surfaces of finite dimensions. *Progress in Heat and Mass Transfer*, Vol. 2, p. 87. Pergamon Press, Oxford (1969).
13. S. N. SINGH and R. C. BIRKEBAK. Laminar free convection from a horizontal infinite strip facing downwards. *ZAMP* **20**, 454–461 (1969).
14. J. V. CLIFTON and A. J. CHAPMAN. Natural-convection on a finite-size horizontal plate. *Int. J. Heat Mass Transfer* **12**, 1573–1584 (1969).
15. T. FUJII, H. HONDA and I. MORIOKA. Natural convection along a downward-facing, uniformly heated, horizontal surface. *Preprints Japan Soc. Mech. Engrs*, No. 700–21, 49–52 (1970).
16. T. AIHARA. Natural convection heat transfer from vertical rectangular-fin arrays (part 2, heat transfer from fin-edges). *Bull. Japan Soc. Mech. Engrs* **13**, 1182–1191 (1970).
17. T. FUJII and H. IMURA. Experimental study of natural convection heat transfer from inclined plates and horizontal plates. *Preprints Japan Soc. Mech. Engrs*, No. 704–10, 1–13 (1970).
18. R. J. FORSTROM and E. M. SPARROW. Experiments on the buoyant plume above a heated horizontal wire. *Int. J. Heat Mass Transfer* **10**, 321–331 (1967).
19. K. BRODOWICZ. An analysis of laminar free convection

around isothermal vertical plate. *Int. J. Heat Mass Transfer* **11**, 201–209 (1968).
20. T. AIHARA and E. SAITO. Measurement of free convection velocity field around the periphery of a horizontal torus, *J. Heat Transfer*, **94C**, 95–98 (1972).
21. E. R. G. ECKERT and R. M. DRAKE, JR., *Heat Mass Transfer*, p. 318. McGraw-Hill, New York (1959).
22. Z. ROTEM, Free convection from heated, horizontal downward-facing plates, *ZAMP* **21**, 472–475 (1970).
23. T. AIHARA and K. HATADA, Problems in determination of heat transfer by Schlieren method. National Technical Report, Matsushita Electric Industrial Co., Japan, 8, 129–135 (1962).
24. R. EICHHORN, An analytical investigation of combined free and forced convections and a new method to measure free convection velocity profiles. Ph.D. Thesis, University of Minesota, 86–97 (1959).
25. E. SCHMIDT, Schlierenaufnahmen des Temperaturfeldes in der Nähe wärmeabgebender Körper, *Forsch. Ing.-Wes.* **3**, 181–189 (1932).

APPENDIX 1

Factors Affecting the Velocity Measurements

The various factors which may affect the velocity measurements by the particle trajectories have been discussed in detail for the case of a vertical plate by Eichhorn [24]. Factors 1–4 in Table 2 present the effects of the respective error factors on the present measurement which the authors have estimated after Eichhorn's way.

Factor 5 for the effect of flow acceleration is estimated as follows: Denoting the horizontal velocities of a particle and fluid at any time τ by u_p and u_a respectively, the equation of motion for a particle in the constantly accelerating flow can be approximately expressed as

$$\frac{du_p}{d\tau} = \frac{18g\mu_a}{\gamma_p d^2}(u_a - u_p), \tag{10}$$

where γ_p is the specific weight of the particle (1148 kg/m^3 according to the authors' measurement), μ_a the fluid viscosity, and d the particle diameter. The solution to equation (10) with the initial condition of $u_p = u_a = 0$ at $\tau = 0$, is

$$u_a - u_p = (b\gamma_p d^2/18g\mu_a)[1 - \exp(-18g\mu_a \tau/\gamma_p d^2)], \tag{11}$$

where b is the acceleration of fluid. Therefore, the relative velocity $(u_a - u_p)$ reaches the maximum value as $\tau \to \infty$. The relevant values listed in Table 2 are the order of the terminal relative-velocity which is estimated from equation (11) by taking 0·22 m/s^2 (the maximum in the present experiment) as the value of b.

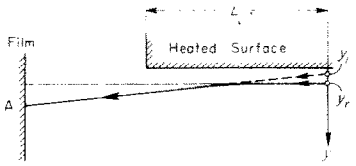

FIG. 20. Schematic representation of deflection of light due to an inhomogeneous temperature field.

By the way, as shown in Fig. 20, if a light emitted by a particle at a position y_r passes through the thermal boundary layer by a distance L parallel to the heated surface, then the light arrives at point A on a film owing to a Schlieren effect as though it was emitted by a particle at a position y_i. This deviation $(y_r - y_i)$ at 760 mm Hg is obtained from the well-known relation [25] as follows:

$$y_r - y_i \doteqdot -\frac{L^2}{2} \cdot \frac{0{\cdot}08}{T_r^2}\left(\frac{\partial\theta}{\partial y}\right)_r, \tag{12}$$

where T_r is the absolute temperature [°K] of fluid at the position y_r. Therefore, the order of the error in determining

Table 2. Effects of various factors on the velocity measurements

Factors	Estimated maximum error	
	Particle dia. = 2μ	Particle dia. = 6μ
1. Settling velocity due to gravity	0·13 mm/s	1·21 mm/s
2. Root mean square distance due to Brownian motion	2·5 μ for 1/8·92 s	1·4 μ for 1/8·92 s
3. Drift due to molecular bombardment	0·15 mm/s	0·15 mm/s
4. Drift due to velocity gradient	2×10^{-9} mm/s	$1{\cdot}4 \times 10^{-7}$ mm/s
5. Terminal relative-velocity of particles in constantly accelerating flow	0·003 mm/s	0·023 mm/s
6. Schlieren effect	0·6%	0·6%
7. Error due to setting situation of a camera	0·5%	0·5%
8. Error in magnification of photograph	1·1%	1·1%
9. Error in slot spacing of a rotating disk shutter	0·5%	0·5%
10. Error in measurement of distance l	0·1 mm	0·1 mm

the particle position y_r from the photograph becomes

$$\frac{(y_i - y_{i0}) - y_r}{y_r} = \frac{0{\cdot}08\,L^2}{2\,y_r}\left[\frac{1}{T_r^2}\left(\frac{\partial\theta}{\partial y}\right)_r - \frac{1}{T_w^2}\left(\frac{\partial\theta}{\partial y}\right)_w\right], \quad (13)$$

with y_{i0} as the corresponding position on the film to the position of $y_r = 0$. The values for Factor 6 listed in Table 2 are the estimated maximum error according to equation (13).

The values for Factors 7–10 in the same table are the respective maximum errors estimated for the present measurement. Summing up the errors for the factors affecting the horizontal velocity measurements, the maximum indeterminant error amounts to about 5·2 per cent.

APPENDIX 2

Buoyant Plume from the Temperature Probe

Figure 21 illustrates a typical buoyant plume from the temperature probe which was first used for measuring the boundary-layer temperatures. This comparatively active buoyant plume is caused primarily by the fact that the bakelite frame of the probe is heated owing to thermal radiation from the lower surface of the test plate. According to the authors' measurement, the surface temperature of the frame exceeded the ambient air temperature by about 1·6°C in case of $\bar{\theta}_w - \theta_\infty \doteqdot 100$°C; the unstable boundary layer near the downward-facing surface is apt to be disturbed even by the existence of such a faint convective motive-force.

CONVECTION NATURELLE LE LONG D'UNE PLAQUE CHAUFFEE HORIZONTALE ET TOURNEE VERS LE BAS

Résumé— On a fait une expérience sur le transfert thermique quasi-bidimensionnel par convection naturelle dans l'air depuis une plaque chauffée horizontale pour un nombre de Rayleigh de l'ordre de 10^7; les champs de vitesse et de température près de la face tournée vers le bas ont été mesurés. On a trouvé que le profil de vitesse est du type écoulement dual et la possibilité d'obtenir des solutions de similarité pour le présent problème est expérimentalement démentie. On traite du domaine pratique de la validité de l'approximation de couche limite et les nombres de Nusselt locaux et moyens sont comparés aux résultats théoriques et expérimentaux rapportés par d'autres auteurs.

FREIE KONVEKTION AN DER UNTERSEITE EINER BEHEIZTEN HORIZONTALEN PLATTE

Zusammenfassung— Der quasi-zweidimensionale Wärmeübergang durch freie Konvektion von einer beheizten, horizontalen Platte an Luft wurde für Rayleigh-Zahlen der Grössenordnung 10^7 experimentell untersucht; die Geschwindigkeits- und Temperaturfelder nahe der nach unten weisenden Oberfläche wurden gemessen. Es zeigte sich, dass das Geschwindigkeitsprofil dem Zweistromtyp entsprach; die Versuche ergaben keine Möglichkeit, für das vorliegende Problem Ähnlichkeitslösungen zu erhalten. Der praktisch erreichbare Bereich für Grenzschichtnäherungslösungen wird diskutiert und die örtlichen und mittlieren Nusselt-Zahlen werden mit theoretischen und experimentellen Ergebnissen anderer Autoren verglichen.

ТЕПЛООБМЕН НА ОБРАЩЕННОЙ ВНИЗ ПОВЕРХНОСТИ ГОРИЗОНТАЛЬНОЙ НАГРЕВАЕМОЙ ПЛАСТИНЫ ПРИ НАЛИЧИИ СВОБОДНОЙ КОНВЕКЦИИ

Аннотация—Проведено экспериментальное исследование квазидвумерного теплообмена при наличии свободной конвекции от нагреваемой горизонтальной пластины при числах Релея порядка 10^7 в воздухе. Измерялись поля температур и скоростей вблизи обращенной вниз поверхности. Найдено, что распределение скорости аналогично распределению, имеющемуся при двойном течении. Экспериментально показано, что для данной задачи нельзя получить автомодельное решение. Рассматривается область практического применения приближения пограничного слоя, а местные и средние числа Нуссельта сравниваются с теоретическими и экспериментальными данными других исследователей.